

Topological state estimation in water distribution systems: Mixed integer quadratic programming approach

Sarai Díaz¹, Roberto Mínguez², and Javier González³

¹Dr. Eng, Dept. of Civil Eng., Univ. of Castilla-La Mancha, Av. Camilo José Cela s/n, 13071 Ciudad Real (Spain). E-mail: Sarai.Diaz@uclm.es.

²Dr. Eng, HIDRALAB INGENIERÍA Y DESARROLLOS, S.L., Spin-Off UCLM, Hydraulics Laboratory Univ. of Castilla-La Mancha, Av. Pedriza, Camino Moledores s/n, 13071 Ciudad Real (Spain). E-mail: roberto.minguez@hidralab.com.

³Dr. Eng, Dept. of Civil Eng., Univ. of Castilla-La Mancha, Av. Camilo José Cela s/n, 13071 Ciudad Real (Spain). // HIDRALAB INGENIERÍA Y DESARROLLOS, S.L., Spin-Off UCLM, Hydraulics Laboratory Univ. of Castilla-La Mancha, Av. Pedriza, Camino Moledores s/n, 13071 Ciudad Real (Spain). E-mail: Javier.Gonzalez@uclm.es.

The final publication is available at

<https://ascelibrary.org/doi/10.1061/%28ASCE%29WR.1943-5452.0000934>

ABSTRACT

State estimation (SE) techniques can be applied to compute the most likely hydraulic state of a water distribution system from the available measurements at a given time. Different approaches exist in the technical literature to undertake such an analysis, but in all of them it is assumed that pump and valve statuses are known beforehand. Such consideration may lead to unrealistic results if real-time unnotified changes in the operation of the network take place, thus limiting the usefulness of the information provided by telemetry systems. This work drops the known-status assumption and presents the concept of *topological state estimation* (TSE), which permits not only to compute the

23 hydraulic state of the system, but also the current pump and valve status according to the existing
24 measurements. More specifically, a novel methodology for TSE is set out in this paper. The
25 proposed method is derived from the original mixed integer non-linear programming formulation
26 of the problem, which is transformed in an iterative mixed integer quadratic programming problem
27 by linearizing some hydraulic constraints. The potential of the methodology is presented by means
28 of an illustrative example and a large case study, where pumps, gate valves and check valves exist.
29 Results show that TSE would successfully contribute to make the most of available telemetry
30 systems, hence expanding the online monitoring possibilities of water distribution networks.

31 **Keywords:** weighted least squares, network topology, monitoring, observability, reliability

32 INTRODUCTION

33 Nowadays, telemetry systems have become essential for the online monitoring of large water
34 distribution networks. Such systems collect real-time data of the metering devices distributed
35 throughout the network, which can eventually be converted into information about its hydraulic
36 state. In this regard, *state estimation* (SE) has been considered as an efficient technique to process
37 available measurements in both power supply (Schweppe and Wildes 1970) and water systems
38 (Coulbeck 1977) for many years. A SE algorithm provides the most likely hydraulic state of
39 a network by minimising the differences between the available measurements and the estimated
40 variables (i.e. pressure, flow and demand) at a given time, which are related to each other by the
41 flow governing equations (Díaz et al. 2016b).

42 SE has been traditionally posed as a weighted least-squares (WLS) problem in the water
43 domain (Bargiela 1984; Brdys and Ulanicki 2002). Nevertheless, alternative approaches have been
44 presented over the years to enhance the performance of the state estimator. On the one hand,
45 Sterling and Bargiela (1984) adapted the weighted least-absolute-values (WLAV) estimation from
46 the power field (Irving et al. 1978) in order to better deal with gross errors, and Powell et al. (1988)
47 even developed a method combining the advantages of WLS and WLAV in one algorithm. On
48 the other hand, Bargiela and Hainsworth (1989) highlighted the importance of evaluating state
49 estimation uncertainty, based on which the so called set-bounded state estimation (SBSE) problem

50 was formulated (Brdys and Chen 1993; Gabrys and Bargiela 1996), and several other uncertainty
51 evaluation strategies were presented (Nagar and Powell 2000; Díaz et al. 2016a). Concurrently,
52 variations of the traditional WLS have been developed with different purposes, such as dealing
53 with low measurement redundancy (Andersen and Powell 2000), introducing measurement bounds
54 in the objective function (Andersen et al. 2001), or using graph theory to reduce the complexity
55 of the problem (Carpentier and Cohen 1991; Kumar et al. 2008). In all of these approaches, the
56 state estimator was applied to a measurement configuration assuming a given network topology,
57 i.e. considering a given pump and valve status configuration. In this paper we denote network
58 topology as the pump and valve status configuration of the system, i.e. its connectivity. This is
59 common practice in water distribution system management in general (Giustolisi et al. 2008), and
60 state estimation applications in particular (Díaz et al. 2017b).

61 However, the status of pumps and valves (i.e. network topology) changes with frequency in
62 water distribution systems to adapt the network to the population needs. Some of these changes are
63 considered normal operation procedures that are required in order to provide high-quality supply at
64 different times. Such is the case of the intentional starting or stopping of a pump, or the deliberate
65 closure of a given valve. Also, the status of pumps and valves in the system can change due to the
66 failure of one of the elements in the network (e.g. pipe burst, pump out of service) or as a response
67 to such failures in order to enhance reliability (Wright et al. 2015), i.e. the ability of the system
68 to perform well in abnormal operation conditions (Goulter 1995). Therefore, even though water
69 utilities are normally aware of some usual operating scenarios, it is difficult to keep record of all
70 the changes that take place in the network topology in real-time applications, i.e. it is complicated
71 to keep an up-to-date hydraulic model of the system. This constitutes a major limitation for the
72 online implementation of SE techniques, as the aforementioned methodologies assumed a given
73 topology that may not exactly simulate the current situation of the water distribution network. It is
74 worth mentioning that if the assumed topology is not consistent with the actual system, SE results
75 may be unrealistic, as measurements provided by telemetry systems correspond to a reality that is
76 different from the hydraulic simulation model.

77 The importance of incorporating changes in the network topology has been discussed before in
78 the context of solving (Giustolisi et al. 2008) and calibrating (Lansey and Basnet 1991; Liberatore
79 and Sechi 2009; Laucelli et al. 2011; Sophocleous et al. 2016) water systems. Also, Díaz et al.
80 (2017b) delved in the possibilities of topological observability analysis in water distribution systems.
81 This approach adapted the traditional observability analysis, which is a prior necessary step to any
82 SE algorithm (Carpentier and Cohen 1991; Díaz et al. 2016), to the possibility of now knowing
83 the pump and valve status beforehand. This method permits to identify not only the hydraulic
84 variables that could be computed in a subsequent SE process, but also the status of which pumps
85 and valves could be inferred from the available measurements. Nevertheless, this analysis only
86 permits to asses if there are sufficient algebraic relationships to infer the pump or valve status from
87 the available measurements, but as measurements are prone to errors, it does not guarantee that the
88 estimated status is correct. When measurement uncertainty is high, sometimes there may not be
89 enough statistical significance to infer the pump or valve status, even if they are observable. To take
90 into account noisy measurements and properly estimate the status of controlling devices, a method
91 for *topological state estimation* (TSE) must be developed.

92 TSE drops the assumption of the network topology being known at each time, enabling to
93 consider that pumps and valves can be either open or closed, and the correct status must be inferred
94 from the available measurements. Therefore, such methodology permits not only to compute
95 the hydraulic state of the system, but also the current network topology by including as many
96 binary variables as the number of pumps and valves that exist in the network. The inclusion
97 of binary variables leads to a mixed integer non-linear programming (MINLP) problem that is
98 difficult to solve, especially when a large number of controlling devices exist in the system. The
99 aim of this work is to present a novel methodology for TSE that transforms such a challenging
100 formulation into an iterative mixed integer quadratic programming (MIQP) problem. The proposed
101 algorithm iteratively linearizes the hydraulic constraints that introduce non-linearity to the problem
102 (i.e. headloss equations and characteristic curves of the pumps in the system) and solves the
103 TSE optimisation problem, which is formed by a quadratic objective function and a set of linear

104 hydraulic constraints. Expressions for the consistent simulation of pumps, gate valves and check
 105 valves are here provided. Moreover, the proposed method permits to take into account that either
 106 the characteristic curve of a pump is known or completely unknown, being possible to estimate the
 107 most likely pumping head even in the latter case. In this study, it is assumed that the number and
 108 location of meters have been previously assessed via topological observability analysis, and the
 109 measurements from the meters were synthetically generated. Also, the hydraulic network model
 110 used in this study has been previously calibrated.

111 The paper is organised as follows: firstly, the formulation of TSE as a MINLP problem is
 112 explained, including a description of the objective function, the general hydraulic constraints and
 113 the specific topological hydraulic constraints required to simulate the presence of pumps and
 114 valves. Then, the adopted solution strategy, which converts the MINLP problem in an iterative
 115 MIQP problem, is provided. The novel methodology is subsequently applied to a small example,
 116 which permits to illustrate the potential of TSE. Afterwards, the C-Town case study is analysed to
 117 prove that the method is robust for larger systems, and finally, relevant conclusions are drawn.

118 **TOPOLOGICAL STATE ESTIMATION**

119 **Problem formulation**

120 *Objective function*

121 The TSE problem can be posed as a non-linear WLS mathematical programming problem with
 122 objective function:

$$123 \quad \underset{h_i; \forall i \in \mathcal{V}}{\text{Minimize}} \left[\sum_{\forall i \in \mathcal{V}_m} \left(\frac{\tilde{h}_i - h_i}{\sigma_i^h} \right)^2 + \sum_{\forall i, j \in \mathcal{L}_m^{\text{PI}}} \left(\frac{\tilde{Q}_{i,j} - Q_{i,j}}{\sigma_{i,j}^Q} \right)^2 + \sum_{\forall i \in \mathcal{V}_m^Q} \left(\frac{\tilde{q}_i - q_i}{\sigma_i^q} \right)^2 \right], \quad (1)$$

124 where the squared difference between existing measurements and estimated variables is to be
 125 minimised. In terms of variables, $h_i; \forall i \in \mathcal{V}$ refers to head levels at all the nodes in the system (\mathcal{V}),
 126 $Q_{i,j}; \forall i, j \in \mathcal{L}^{\text{PI}}$ is the water flow through the pipe elements in the system (\mathcal{L}^{PI}), and $q_i; \forall i \in \mathcal{V}^Q$
 127 is the water consumption at demand nodes (\mathcal{V}^Q). On the other hand, variables overlined with
 128 a tilde represent the value of the measurement in the subset of nodes and pipes where variables

129 are measured. Therefore, \mathcal{V}_m , $\mathcal{L}_m^{\text{PI}}$ and \mathcal{V}_m^{Q} represent the subset of nodes where head levels are
 130 measured, the subset of pipes where flows are metered, and the subset of nodes where water demands
 131 are measured, respectively. Consequently, $\sigma_i^h; \forall i \in \mathcal{V}_m$, $\sigma_{i,j}^Q; \forall i, j \in \mathcal{L}_m^{\text{PI}}$, and $\sigma_i^d; \forall i \in \mathcal{V}_m^{\text{Q}}$ are
 132 the standard deviations for measurements of head, flow and demand, respectively. Variables and
 133 measurements are independent of time t all along this work because a pseudo-static approach is
 134 considered for TSE, i.e. flow is steady and each estimation can be understood as an instantaneous
 135 snapshot of the system. Also, it must be highlighted that only measurement uncertainty is taken
 136 into account in Eq. (1). This is the traditional scope for state estimation methodologies, which
 137 normally assume that the hydraulic model (e.g. pipe infrastructure information, tank dimensions)
 138 has been previously calibrated (Díaz et al. 2016).

139 At this point, it is important to identify the state variables of the problem, which are the
 140 minimum set of variables that enable to characterise the hydraulic state of the system. Note that if
 141 the status of pumps and valves is known, nodal heads can be considered the state variables of the
 142 system, as any combination of head levels leads to a certain and credible flow solution (Díaz et al.
 143 2016). However, if some of the statuses of pumps and valves are unknown, the state variable set
 144 must also include the unknown binary variables, without which the state of the system cannot be
 145 fully defined. As it will be presented later on, binary variables enable to simulate that pumps and
 146 valves can either be open or closed, and the TSE algorithm must determine their status based on
 147 the existing measurements. Once state variables are computed, the rest of variables (i.e. flows and
 148 demands) can be inferred thanks to the rest of hydraulic constraints, which are now presented.

149 *Hydraulic constraints*

150 In this work, the Hazen-Williams headloss equation is assumed all along:

$$151 \quad h_i - h_j = K_{i,j} Q_{i,j} |Q_{i,j}|^{c-1}; \forall i, j \in \mathcal{L}^{\text{PI}}, \quad (2)$$

152 where $K_{i,j}$ is the flow resistance pipe coefficient, $c = 1.852$ is the Hazen-Williams exponent and
 153 h_i and h_j refer to the head levels at the initial and final nodes of the pipeline. Note that adopting

154 the Darcy-Weisbach equation instead of the Hazen-Williams approach would require calculation
 155 of the friction factor from an implicit function. Therefore, and even though the Hazen-Williams
 156 formula for pipe head loss applies over a limited range of flows, it is a common choice in the field
 157 because its explicit formulation is easy to compute (Eck and Mevissen 2012). In this work, flow
 158 is taken as positive when water moves from the lower to the higher numbering node. For each
 159 node, two subsets can be defined. Ω_i^O contains the water outflows from node i to the rest of nodes
 160 $j > i$ connected to i with a pipe. On the other hand, Ω_i^I corresponds to the inflows to node i from
 161 the rest of nodes $j < i$ connected to i . Note that the head level can be estimated from the node
 162 elevation and pressure. However, as pumps and valves must be included in the hydraulic model for
 163 TSE purposes, computation of the head level at each node must also take into account the energy
 164 provided by pump elements ($\forall i, j \in \mathcal{L}^P$, being \mathcal{L}^P the set of all pumps in the network):

$$165 \quad h_i = e_i + p_i + \sum_{k,l \in \mathcal{L}^P} \delta_{i,k,l} h_{k,l}^P; \forall i \in \mathcal{V}, \quad (3)$$

166 where $e_i; \forall i \in \mathcal{V}$ is the elevation at the node (considered a constant parameter), and $p_i; \forall i \in \mathcal{V}$
 167 is its pressure, being \mathcal{V} the set of all nodes in the network. The following summand refers to the
 168 pumping head $h_{k,l}^P; \forall k, l \in \mathcal{L}^P$ that any pump can inject at a specific node. If node i is the final node
 169 of a given pump $k, l \in \mathcal{L}^P$, then Kronecker delta $\delta_{i,k,l}$ is equal to one, and the pumping head must
 170 be added. The open/closed status of the pump is later on introduced in the formulation through
 171 topological hydraulic constraints. Gate valves and check valves are also considered in this paper,
 172 but they are not included in Eq. (3) because we assume that there is no headloss through them, as
 173 it will be presented afterwards.

174 The continuity equation can be written as:

$$175 \quad q_i = - \sum_{j \in \Omega_i^I} Q_{i,j} + \sum_{j \in \Omega_i^O} Q_{i,j}; \forall i \in (\mathcal{V}^Q \cup \mathcal{V}^T), \quad (4)$$

176 where q_i is negative at demand nodes ($\forall i \in \mathcal{V}^Q$, being \mathcal{V}^Q the subset of demand nodes) and null

177 at the so called transit nodes ($\forall i \in \mathcal{V}^T$, being \mathcal{V}^T the subset of transit nodes). Note that Eq. (4) is
 178 only applied at demand and transit nodes, because in a pseudo-static estimation tanks and reservoirs
 179 can be represented by only their head level. An additional condition is in fact that water demand at
 180 transit nodes is zero:

$$181 \quad q_i = 0; \forall i \in \mathcal{V}^T. \quad (5)$$

182 Physical limits must also be defined for pipe and node elements as follows:

$$183 \quad Q_{i,j} \leq Q_{i,j}^{max}; \forall i, j \in \mathcal{L}^{PI} \quad (6)$$

$$184 \quad -Q_{i,j} \leq Q_{i,j}^{max}; \forall i, j \in \mathcal{L}^{PI} \quad (7)$$

$$185 \quad h_i \leq h_i^{max}; \forall i \in \mathcal{V} \quad (8)$$

$$186 \quad h_i \geq h_i^{min}; \forall i \in \mathcal{V}, \quad (9)$$

187 where Eqs. (6)-(7) impose a maximum $Q_{i,j}^{max}$ for the absolute value of the water flow through
 188 pipes, and Eqs. (8)-(9) establish a maximum (h_i^{max}) and minimum (h_i^{min}) value for head levels,
 189 respectively.

193 *Topological hydraulic constraints: pumps*

194 Specific expressions must also be derived for pump elements ($\forall i, j \in \mathcal{L}^P$), which are here
 195 treated as link elements of zero length whose end nodes are at the same elevation. These elements
 196 can be either open or closed, and the on/off (i.e. 1/0) status of each pump is taken into account
 197 by introducing a binary variable for each existing pump $b_{i,j}^P; \forall i, j \in \mathcal{L}^P$. To derive the hydraulic
 198 constraints of such elements, two situations must be distinguished beforehand. Pumps only admit a
 199 predefined unidirectional flow (i.e. there is no possibility of having reverse flow through a pump),
 200 but this unidirectional flow can either be of positive or negative sign for a specific pump according
 201 to the aforementioned sign criterion. Therefore, we need to differentiate two subsets $\forall i, j \in \mathcal{L}_+^P$ and
 202 $\forall i, j \in \mathcal{L}_-^P$ in order to correctly simulate that a particular device is pumping water in the positive

203 or negative direction of flow, respectively. Figure 1 shows that there is a $h_{i,j}^P$ increase of pressure at
 204 node j when the device is located to pump water in the positive direction of flow (from i to j), but
 205 this additional energy is applied to the initial node i in devices that pump the water in the negative
 206 direction (from j to i). In addition to this classification, two types of pumps are differentiated in
 207 this work attending to the available information about the pump: pumps with known characteristic
 208 curve ($\forall i, j \in \mathcal{L}_K^P$, being \mathcal{L}_K^P the subset of pump links with known characteristic curve), and pumps
 209 with unknown characteristic curve ($\forall i, j \in \mathcal{L}_U^P$, being \mathcal{L}_U^P the subset of pump links with unknown
 210 characteristic curve). This distinction is made because even though manufacturers normally provide
 211 the characteristic curve for each pump at the time of sale, some network operators know nothing
 212 about the characteristic curve of some pumps, for example if they are working on a longstanding
 213 and/or undocumented water system. As presented by Díaz et al. (2017b), when the characteristic
 214 curve of the pump is available, a known relationship exists between the pumping head and the
 215 circulating flow, thus the curve can be introduced as a constraint and no additional information
 216 is required to characterise the system. On the contrary, if the characteristic curve of the pump is
 217 unknown, an additional unknown is added to the problem, and thus more measurements are needed
 218 to guarantee the system observability.

219 According to this classification, two independent pairs of subsets exist for the general pump
 220 set \mathcal{L}^P : subsets \mathcal{L}_+^P and \mathcal{L}_-^P account for the flow direction through the pump, i.e. $\mathcal{L}^P \equiv \mathcal{L}_+^P \cup \mathcal{L}_-^P$
 221 and $\mathcal{L}_+^P \cap \mathcal{L}_-^P \equiv \emptyset$, whereas subsets \mathcal{L}_K^P and \mathcal{L}_U^P indicate the available information about the
 222 characteristic curve of the element, i.e. $\mathcal{L}^P \equiv \mathcal{L}_K^P \cup \mathcal{L}_U^P$ and $\mathcal{L}_K^P \cap \mathcal{L}_U^P \equiv \emptyset$. Therefore, the hydraulic
 223 constraints related to pump elements can be defined as:

$$224 \quad h_{i,j}^P \geq 0; \forall i, j \in \mathcal{L}^P \quad (10)$$

$$225 \quad -M(1 - b_{i,j}^P) \leq p_i - p_j \leq M(1 - b_{i,j}^P); \forall i, j \in \mathcal{L}^P \quad (11)$$

$$226 \quad Q_{i,j} \leq Q_{i,j}^{max} b_{i,j}^P; \forall i, j \in \mathcal{L}_+^P \quad (12)$$

$$227 \quad Q_{i,j} \geq Q_{i,j}^{min} b_{i,j}^P; \forall i, j \in \mathcal{L}_+^P \quad (13)$$

$$-Q_{i,j} \leq Q_{i,j}^{max} b_{i,j}^P; \forall i, j \in \mathcal{L}_-^P \quad (14)$$

$$-Q_{i,j} \geq Q_{i,j}^{min} b_{i,j}^P; \forall i, j \in \mathcal{L}_-^P \quad (15)$$

$$h_{i,j}^P = \left(A_{i,j}(Q_{i,j})^2 + B_{i,j}|Q_{i,j}| + C_{i,j} \right) b_{i,j}^P; \forall i, j \in \mathcal{L}_K^P \quad (16)$$

$$h_{i,j}^P \leq h_{i,j}^{P,max} b_{i,j}^P; \forall i, j \in \mathcal{L}_U^P, \quad (17)$$

where $A_{i,j}, B_{i,j}, C_{i,j}; \forall i, j \in \mathcal{L}_K^P$ are the parameters of the characteristic curve of each pump, M is a large enough positive constant, and $b_{i,j}^P$ is the binary variable at pump link from node i to node j . Eq. (10) forces the pumping head to be positive no matter the scenario, because a pump always supplies energy to the system regardless of the injection point (see Figure 1). Constraint (11) forces the pressure at each side of the pump to be the same when the pump is open ($b_{i,j}^P = 1$), but it permits a hydraulic disconnection between nodes i and j when the pump is closed ($b_{i,j}^P = 0$), i.e. p_i and p_j can be significantly different when there is no flow through the pump. Hence, constant M must be large enough to model the difference in pressure head between nodes. Eqs. (12)-(13) determine the maximum ($Q_{i,j}^{max}$) and minimum ($Q_{i,j}^{min}$) flow through pumps in which the water moves from node i to node j , and Eqs. (14)-(15) are analogous for elements with negative flow. Constraint (16) provides the characteristic curves when they are available, forcing the pumping head to be null when the pump is closed. Similarly, Eq. (17) enables the pumping head to reach a pre-set maximum value $h_{i,j}^{P,max}; \forall i, j \in \mathcal{L}_U^P$ when information about the characteristic curve is not available, and fixes the pumping head to zero when the pump is not working.

Topological hydraulic constraints: gate valves

Gate valves enable isolation of different segments and/or areas within a given water distribution system. These controlling devices only have two positions, which are represented in this work by binary variables $b_{i,j}^{GV}; \forall i, j \in \mathcal{L}^{GV}$, i.e. $b_{i,j}^{GV} = 1$ when they are open, and $b_{i,j}^{GV} = 0$ when they are closed, being \mathcal{L}^{GV} the subset of gate valve links. As assumed with the pumps, valves are introduced in the hydraulic model as elements of zero length whose nodes keep the same elevation. In this particular case, we assume that there is no headloss through such valves when they are fully open.

259 Hence, the only constraints are:

$$260 \quad -M(1 - b_{i,j}^{GV}) \leq h_i - h_j \leq M(1 - b_{i,j}^{GV}); \forall i, j \in \mathcal{L}^{GV} \quad (18)$$

$$261 \quad Q_{i,j} \leq Q_{i,j}^{max} b_{i,j}^{GV}; \forall i, j \in \mathcal{L}^{GV} \quad (19)$$

$$262 \quad -Q_{i,j} \leq Q_{i,j}^{max} b_{i,j}^{GV}; \forall i, j \in \mathcal{L}^{GV}. \quad (20)$$

263 Eq. (18) ensures that the energy gradient is zero when the valve is open (i.e. no energy losses), and
 264 enables h_i and h_j to differ when the valve is closed. This expression is analogous to Eq. (11) for
 265 pumps, because as the elevation at end nodes is the same in gate valves and no losses are assumed
 266 $h_i - h_j = p_i - p_j$. Analogously to the pump case, constant M must be large enough to model the
 267 difference in pressure head between nodes. Eqs. (19)-(20) establish that the absolute value of flow
 268 through the valve must be lower than the maximum allowed in the network. Hence, if the valve is
 269 closed, $b_{i,j}^{GV} = 0$ and the flow through the pipe is zero.

270 *Topological hydraulic constraints: check valves*

271 Check valves are placed in water distribution systems with the aim of avoiding inverse flows
 272 (Deuerlein et al. 2009). Consequently, they are directional devices that require the allowed direction
 273 of flow to be defined beforehand. As with pumps, the general set for check valves ($\forall i, j \in \mathcal{L}^{CV}$)
 274 must then be divided in two subsets: \mathcal{L}_+^{CV} when the water is only allowed to move from the lower to
 275 the higher numbering node, and \mathcal{L}_-^{CV} if only negative flow is allowed, with $\mathcal{L}^{CV} \equiv \mathcal{L}_+^{CV} \cup \mathcal{L}_-^{CV}$ and
 276 $\mathcal{L}_+^{CV} \cap \mathcal{L}_-^{CV} \equiv \emptyset$. The following constraints are required to simulate the status $b_{i,j}^{CV}; \forall i, j \in \mathcal{L}^{CV}$ of
 277 such controlling devices:

$$278 \quad -M(1 - b_{i,j}^{CV}) \leq h_i - h_j \leq M(1 - b_{i,j}^{CV}); \forall i, j \in \mathcal{L}^{CV} \quad (21)$$

$$280 \quad Q_{i,j} \leq Q_{i,j}^{max} b_{i,j}^{CV}; \forall i, j \in \mathcal{L}_+^{CV} \quad (22)$$

$$281 \quad -Q_{i,j} \leq Q_{i,j}^{max} b_{i,j}^{CV}; \forall i, j \in \mathcal{L}_-^{CV} \quad (23)$$

285

$$286 \quad Q_{i,j} \geq 0; \forall i, j \in \mathcal{L}_+^{CV} \quad (24)$$

287

$$288 \quad -Q_{i,j} \geq 0; \forall i, j \in \mathcal{L}_-^{CV}. \quad (25)$$

289 Eqs. (21)-(23) are equivalent to (18)-(20) for gate valves, i.e. it is assumed that no energy loss
 290 occurs when the valve is open and maximum values of flow are established. Eqs. (24)-(25) force the
 291 water to move in the positive and negative direction, respectively, and impose null flow otherwise.

292 **Solution methodology**

293 Eqs. (1)-(25) define the MINLP problem required to implement TSE in any water distribution
 294 system. More specifically, Eqs. (1)-(9) set out the traditional non-linear programming (NLP)
 295 problem for SE, which is then complemented with hydraulic constraints that simulate the presence
 296 of pumps, gate valves and check valves. Therefore, if the status of pumps and valves is known
 297 beforehand thanks to a good monitoring or the installation of position sensors in controlling devices,
 298 binary variables can be considered fixed, and problem (1)-(25) can be treated as a NLP problem.
 299 However, as the network topology is not likely to be fully known in large systems, and the objective
 300 of TSE is to infer both the hydraulic state and the pump/valve status of the system from a set of
 301 available measurements, TSE must be generally addressed as a MINLP problem.

302 Developing robust solution methodologies for MINLP problems is a challenging issue at present,
 303 and their computational implementation is expected to experience a significant rise in the years to
 304 come (Berthold 2014). Even though various solvers are commercially available to solve MINLP
 305 problems, their suitability highly depends on each particular problem, especially if the problem is
 306 nonconvex (Bussieck and Vigerske 2011), as it is the case of TSE. As selecting a reliable and robust
 307 solver that works well in different networks is not straightforward, the original MINLP problem
 308 is transformed in this work into an iterative MIQP problem. The change from MINLP to MIQP
 309 requires to linearize the non-linear equations of problem (1)-(25), i.e. the headloss equation and the
 310 characteristic curves associated with pumps. Note that linearizing the Hazen-Williams equation is
 311 not a novel idea, and a literature review can be found in Eck and Mevissen (2012). For example,

312 a piecewise linearization for Eqs. (2) and (16) could be adopted. However, this strategy implies a
 313 significant increase in the number of binary variables in order to accurately represent the curvature
 314 of such non-linear functions (Morsi et al. 2012). Alternatively, a successive linearization strategy
 315 is here adopted. It is true that linearization may lead to instabilities along the iterative process, but
 316 as the algorithm is conceived for on-line state estimation, it is likely to run with a pre-specified
 317 frequency. Therefore, major simultaneous changes are not expected from one state estimation to
 318 the next. This enables the state estimation problem to be initialised from the previous result, i.e. the
 319 linearization occurs around a point which is reasonably close to the estimated flow scenario. Once
 320 Eqs. (2) and (16) are linearized, the objective function remains as the only non-linearity of problem
 321 (1)-(25), thus the optimisation problem can be solved with a MIQP approach. Current state-of-
 322 the-art MIQP solvers, such as *CPLEX* ([www-01.ibm.com/software/commerce/optimization/cplex-](http://www-01.ibm.com/software/commerce/optimization/cplex-optimizer)
 323 [optimizer](http://www-01.ibm.com/software/commerce/optimization/cplex-optimizer)) or *Gurobi* (www.gurobi.com), can solve this type of problems very efficiently. In any
 324 case, the problem linearization comes at the cost of an iterative algorithm, which will be presented
 325 once the linear versions of the aforementioned equations are posed.

326 Eq. (2) can be linearized around an initial flow $Q_{0,i,j}; \forall i, j \in \mathcal{L}^{\text{PI}}$ as follows:

$$327 \quad h_i - h_j = (1 - c)K_{i,j}|Q_{0,i,j}|^{c-1}Q_{0,i,j} + K_{i,j}c|Q_{0,i,j}|^{c-1}Q_{i,j}; \forall i, j \in \mathcal{L}^{\text{PI}}. \quad (26)$$

328 Similarly, the characteristic curve of any pump (Eq. (16)) can be linearized with respect to
 329 $Q_{0,i,j}; \forall i, j \in \mathcal{L}_K^{\text{P}}$ as:

$$330 \quad h_{i,j}^{\text{P}} = [C_{i,j} - A_{i,j}(Q_{0,i,j})^2 + (2A_{i,j}|Q_{0,i,j}| + B_{i,j}) \text{sign}(Q_{0,i,j})Q_{i,j}] b_{i,j}^{\text{P}}; \forall i, j \in \mathcal{L}_K^{\text{P}}, \quad (27)$$

331 however, as the characteristic curve is affected by the binary variable $b_{i,j}^{\text{P}}; \forall i, j \in \mathcal{L}_K^{\text{P}}$, the previous
 332 expression is still non-linear. In order to provide a linear alternative to Eq. (16), Eq. (27) can be
 333 linearized as follows:

$$334 \quad h_{i,j}^{\text{P},\text{min}} b_{i,j}^{\text{P}} \leq h_{i,j}^{\text{P}} \leq h_{i,j}^{\text{P},\text{max}} b_{i,j}^{\text{P}}; \forall i, j \in \mathcal{L}_K^{\text{P}} \quad (28)$$

$$h_{i,j}^{P,min}(1-b_{i,j}^P) \leq C_{i,j}-A_{i,j}(Q_{0,i,j})^2+(2A_{i,j}|Q_{0,i,j}|+B_{i,j}) \text{sign}(Q_{0,i,j})Q_{i,j}-h_{i,j}^P \leq h_{i,j}^{P,max}(1-b_{i,j}^P); \forall i, j \in \mathcal{L}_K^P, \quad (29)$$

where $h_{i,j}^{P,min}; \forall i, j \in \mathcal{L}_K^P$ and $h_{i,j}^{P,max}; \forall i, j \in \mathcal{L}_K^P$ have been introduced as parameters, and represent the minimum and maximum pumping head at pump link from node i to node j . Hence, when the pump is closed ($b_{i,j}^P = 0$), Eq. (28) fixes the pumping head to zero, and when the pump is open ($b_{i,j}^P = 1$), Eq. (29) forces $h_{i,j}^P$ to the linearized characteristic curve, i.e. Eqs. (28)-(29) are equivalent to Eq. (27).

Therefore, the MINLP problem (1)-(25) can be formulated as the MIQP problem (1), (3)-(15), (17)-(26), (28)-(29), which incorporates the linearized Hazen-Williams headloss equations and characteristic curves (if known). In this paper, the *CPLEX* solver is used to solve such problem for a given initialisation. As state estimation techniques are normally fed with online telemetry data, the initial value for $Q_{0,i,j}; \forall i, j \in (\mathcal{L}^{PI} \cup \mathcal{L}_K^P)$ can be obtained from the previous TSE, or from any other flow scenario in the system. Then, the MIQP solution must be used as initialisation for the following iteration, enabling a linearization that is progressively closer to the optimal solution. In order to speed convergence and enhance stability, a sub-relaxation method is here adopted when the iteration number k exceeds a selected value k_{lim} :

$$\begin{cases} Q_{0,i,j}^{(k+1)} = Q_{i,j}^{(k)} & \text{if } k \leq k_{lim} \\ Q_{0,i,j}^{(k+1)} = Q_{i,j}^{(k)}\lambda + (1-\lambda)Q_{0,i,j}^{(k)} & \text{if } k_{lim} < k < k_{max}, \end{cases} \quad (30)$$

with $k_{lim} = 10$. The maximum number of iterations and the subrelaxation factor are set out as $k_{max} = 100$ and $\lambda = 0.3$, respectively, all along this work. The iterative algorithm (summarised in Figure 2) finishes when the relative error of the objective function between successive iterations becomes lower than a specified tolerance, which is considered 10^{-6} in this paper. Then, the algorithm can be formally written as follows:

Algorithm 1 *MIQP approach for TSE*

Input: *Measurements and standard deviation of measurements, model parameters, available infor-*

359 *mation of pumps, flow direction in pumps and check valves, and $Q_{0,i,j}; \forall i, j \in (\mathcal{L}^{\text{PI}} \cup \mathcal{L}^{\text{P}})$, which*
 360 *can be obtained from a previous TSE result or from any other flow scenario in the system.*

361 **Step 1: Solve MIQP problem.** *The linearized MIQP problem (1), (3)-(15), (17)-(26), (28)-(29) is*
 362 *solved for $Q_{0,i,j}; \forall i, j \in (\mathcal{L}^{\text{PI}} \cup \mathcal{L}^{\text{P}})$.*

363 **Step 2: Check tolerance.** *If the relative error of the objective function is lower than 10^{-6} continue*
 364 *with step 3, otherwise, update the iteration counter $k \rightarrow k + 1$, update $Q_{0,i,j}; \forall i, j \in (\mathcal{L}^{\text{PI}} \cup \mathcal{L}^{\text{P}})$*
 365 *according to Eq. (30), and continue with step 1.*

366 **Step 3: Output.** *Estimated head levels at nodes $\hat{h}_i; \forall i \in \mathcal{V}$, water flows through link elements*
 367 *$\hat{Q}_{i,j}; \forall i, j \in \mathcal{L}$ with $\mathcal{L} = \{\mathcal{L}^{\text{PI}}, \mathcal{L}^{\text{P}}, \mathcal{L}^{\text{GV}}, \mathcal{L}^{\text{CV}}\}$, demands at junction nodes $\hat{q}_i; \forall i \in \mathcal{V}^{\text{Q}}$, and binary*
 368 *variables for pumps $\hat{b}_{i,j}^{\text{P}}; \forall i, j \in \mathcal{L}^{\text{P}}$, gate valves $\hat{b}_{i,j}^{\text{GV}}; \forall i, j \in \mathcal{L}^{\text{GV}}$ and check valves $\hat{b}_{i,j}^{\text{CV}}; \forall i, j \in \mathcal{L}^{\text{CV}}$.*

369 This algorithm at present is heuristic, since it cannot be assured that a global solution of the
 370 original MINLP problem has been achieved. Nevertheless, the algorithm proposed in the paper
 371 presents good convergence properties and, as it will be shown in the following examples, it is com-
 372 putationally efficient. As opposed to other approximate methods lacking rigorous grounding, such
 373 as genetic algorithms or simulated annealing, the proposed solution approach is a mathematically
 374 sound heuristic based on the application of a well-known optimization technique.

375 ILLUSTRATIVE EXAMPLE

376 The small water system presented by Díaz et al. (2017b) is used as an illustration in this
 377 paper. Figure 3 provides the network layout, in which 6 junctions and 2 reservoirs are connected
 378 to each other through 7 pipes, a gate valve and a pump. TSE is here undertaken considering
 379 two different scenarios in what regards the available information about the pump: (1) the pump
 380 has a characteristic curve defined by $A_{6,8} = -2.2204 \cdot 10^{-16} \text{ h}^2/\text{m}^5$, $B_{6,8} = -0.3126 \text{ h}/\text{m}^2$ and
 381 $C_{6,8} = 125.2806 \text{ m}$, and (2) there is no information whatsoever about the characteristic curve of
 382 the pump. Also, we assume that water levels at both reservoirs are metered, water demands at all
 383 nodes are pseudomeasured, and a number of flow meters exist. As shown in Figure 3, two settings
 384 of flow meters are considered in this example for the sake of comparison: a first set of three flow

385 meters located in pipes 1-2, 3-7 and 2-5, and a second set of four flow meters located in pipes 1-2,
 386 3-7, 2-5 and 4-8. It must be highlighted that all measurement configurations have been previously
 387 assessed with a topological observability analysis (Díaz et al. 2017b), which is a prior necessary
 388 step to TSE. Such an analysis enables to guarantee that there are enough algebraic relationships to
 389 infer the hydraulic variables and the pump and valve statuses from the available measurements.

390 Since the method is heuristic, we have to check its performance under a controlled setting,
 391 and for this reason, measurements at each of such locations are synthetically generated in this
 392 work, i.e. sampling experiments are undertaken. With this purpose, a known pump/valve status
 393 is assumed (e.g. both the valve and the pump are considered opened), and the flow network
 394 solution is computed. Then, 1000 measured values are synthetically generated for each of the
 395 available measurements by considering a random variable distribution with mean equal to the
 396 corresponding flow, head or demand value obtained from solving the flow network, and a standard
 397 deviation. It must be highlighted that even though we assume a network topology to generate the
 398 measurements, pump/valve binary variables are freed before running the TSE algorithm in order to
 399 test the ability of the method to correctly determine the network topology. The standard deviations
 400 assumed for each type of measurement are $\sigma_i^h = 0.01 \text{ m}; \forall i \in \mathcal{V}_m$, $\sigma_i^q = 20\% \bar{q}_i; \forall i \in \mathcal{V}_m^Q$
 401 and $\sigma_{i,j}^Q = \sqrt{\frac{1}{6} + (2\% \bar{Q}_{i,j})^2}; \forall i, j \in \mathcal{L}_m^{\text{PI}}$, where \bar{q}_i and $\bar{Q}_{i,j}$ represent the value of demand and flow
 402 variables in the flow network solution. It is worth mentioning that a greater uncertainty is introduced
 403 in each demand because we assume that water consumptions are pseudomeasured, i.e. estimated
 404 from historic data, as it may be the case in a real water system (Bargiela and Hainsworth 1989). On
 405 the other hand, $\sigma_{i,j}^Q$ is constituted by a fixed uncertainty of $\frac{1}{\sqrt{6}}$ that comes from considering that flow is
 406 metered as volume in m^3 and the difference in volume over time provides a measurement of flow, and
 407 a variable term that depends on the water flow itself, as it normally occurs in real flow meters. Once
 408 measurements have been computed, Monte Carlo simulations are undertaken: the TSE problem
 409 is solved considering each of the 1000 artificially generated measurements/pseudomeasurements.
 410 The process is repeated for all different combinations of pump and valve status: open valve-open
 411 pump, open valve-closed pump, closed valve-open pump, and closed valve-closed pump. In all

412 of these cases the algorithm for TSE described in Figure 2 is initialised $Q_{0,i,j}; \forall i, j \in (\mathcal{L}^{\text{PI}} \cup \mathcal{L}^{\text{P}})$
 413 from the flow network solution associated with an open valve and pump, which is here subjected
 414 to a 5% noise to avoid straightforward solutions when open valve-open pump is the real network
 415 topology. This permits to evaluate to what extent the methodology presented in this paper permits
 416 to detect changes in the network topology. Note that synthetic measurements are here used to test
 417 the algorithm, or otherwise you need a real network with a huge set of metering devices in order to
 418 use some of them for validation.

419 Now, TSE results considering the characteristic curve of the pump known and unknown are
 420 presented. We assume $Q_{i,j}^{\text{max}} = 10 \text{ m/s} \cdot S_{i,j}; \forall i, j \in \mathcal{L}$, $h_i^{\text{max}} = \max(h_i^{\text{max}}) + 200 \text{ m}; \forall i \in \mathcal{V}$,
 421 $h_i^{\text{min}} = -h_i^{\text{max}}; \forall i \in \mathcal{V}$, $M = 300$, $Q_{i,j}^{\text{min}} = 0.01 \text{ m/s} \cdot S_{i,j}; \forall i, j \in \mathcal{L}^{\text{P}}$, $h_{i,j}^{\text{P,max}} = 200 \text{ m}; \forall i, j \in \mathcal{L}^{\text{P}}$
 422 and $h_{i,j}^{\text{P,min}} = 0 \text{ m}; \forall i, j \in \mathcal{L}^{\text{P}}$ all along this paper, where $S_{i,j}$ is the pipe cross-sectional area.

423 **Known characteristic curve**

424 Table 1 provides the TSE results of Monte Carlo simulations when the characteristic curve of
 425 the pump is known. For each of the four network topologies assumed, the percentage of success
 426 in estimating the pump status (S_P), the percentage of success in estimating the gate valve status
 427 (S_{GV}), the average number of iterations required for the TSE algorithm to converge (\bar{k}), and the
 428 maximum number of iterations required to achieve convergence ($\max(k)$) are provided for the two
 429 measurement settings in which 3 and 4 flow meters exist. Additionally, this table gives the average
 430 of the mean squared error in terms of flows (\overline{MSE}) for the 1000 simulations, and the time needed by
 431 the Monte Carlo method to converge in an Intel(R) Core(TM) i7-6700 CPU 3.40 GHz 16GB RAM
 432 desktop computer. The mean squared error for each of the measurement configurations considered
 433 for the analysis can be computed as:

$$434 \quad MSE = \frac{1}{n_L} \sum_{\forall i,j \in \mathcal{L}} (\hat{Q}_{i,j} - \bar{Q}_{i,j})^2, \quad (31)$$

435 with $n_L = 9$ link elements in the illustrative network. Eq. (31) provides the mean squared difference
 436 between the estimated flows ($\hat{Q}_{i,j}; \forall i, j \in \mathcal{L}$) and the real values in the system, which correspond to

437 their values in the corresponding flow network solution $\bar{Q}_{i,j}; \forall i, j \in \mathcal{L}$. Therefore, its average over
438 1000 simulations provides an insight of how much TSE results differ from the real network state.

439 Beginning with the results obtained for the 3 flow meters measurement configuration, the success
440 in estimating the gate valve status (S_{GV}) is 100% no matter the real network state. This is fully
441 expected because of the fact that all inflows and outflows to the valve are metered. Nevertheless,
442 S_P ranges between 61.8 and 92.0% depending on the network topology. This can be explained by
443 the fact that only water level meters and demand pseudomeasurements are available near the pump
444 location, and this does not seem to be enough to correctly estimate the pump status in all cases. As
445 presented by Díaz et al. (2017b), measurement noise may lead to an incorrect status determination
446 during TSE even if the variable has been identified as observable in a prior observability analysis.
447 This is due to the fact that this analysis only considers the number and location of meters, but
448 measurement uncertainty can only be taken into account through TSE itself. We want to highlight
449 that this is not a limitation of the TSE algorithm, as it provides the best possible estimation by taking
450 into account the available noisy measurements. It has been verified that if measurements were exact,
451 a 100% success would be obtained for both the gate valve and the pump in all cases. However,
452 real water systems are subjected to noise, and this affects the capability of the algorithm to detect
453 changes in the pump/valve status. This reality can be counteracted with the addition of metering
454 devices. Table 1 shows that S_P increases to 100% in all scenarios when an additional flow meter is
455 located in pipe 4-8, i.e. this measurement configuration would permit to guarantee that the pump
456 and valve status could be correctly detected regardless of the high uncertainty of the measurements
457 and pseudomeasurements, where uncertainty is particularly important. Consequently, \overline{MSE} is
458 reduced by one order of magnitude when a fourth flow meter is added.

459 In what regards the number of iterations, \bar{k} varies between 2 and 7 depending on the original
460 network state. Note that when both devices are closed, the method converges in few iterations, as
461 it is easy for the algorithm to detect that the pump is closed if the characteristic pump is available.
462 Finally, it must be highlighted that the mean convergence time required for each simulation to
463 converge is between 2 and 3 seconds in all cases.

464 **Unknown characteristic curve**

465 Table 2 provides the same results when the characteristic curve of the pump is unknown. As it
466 happened before, $S_{GV} = 100\%$ in all cases no matter the number of flow meters installed. On the
467 contrary, S_P changes depending on the real network state. As information about the characteristic
468 curve is no longer available, it is expected that the success in the estimation of the correct pump
469 status reduces with respect to the previous scenario. Such is the case of open valve-closed pump
470 and closed valve-closed pump cases when either 3 or 4 flow meters exist. Nevertheless, S_P values
471 in Table 2 are improved with respect to those in Table 1 in the open valve-open pump and closed
472 valve-open pump cases when three flow meters are adopted. This result is not intuitive, but can
473 be explained: by removing the information about the characteristic curve of the pump, we allow
474 the TSE algorithm to estimate the head gain and flow through the pump freely, i.e. no specific
475 relationship is required between $h_{6,8}^P$ and $Q_{6,8}$ and they are both independently adjusted to minimise
476 the objective function. Therefore, the method is correctly identifying the pump/valve status at the
477 cost of failing to accurately estimate the rest of the hydraulic variables in the system, which are no
478 longer subjected to a $h - Q$ constraint in the proximity of the pump. Consequently, \overline{MSE} values are
479 increased from Table 1 to Table 2, as the estimated flows and the real water flows differ considerably
480 regardless of the improvement in the network topology estimation.

481 In what regards the number of iterations, the loss of information about the characteristic curve
482 of the pump negatively affects the speed of the method in this example. Table 2 shows that even
483 $\max(k) = k_{max} = 100$ is reached in some cases, which considerably burdens \bar{k} . More specifically,
484 100 iterations have been achieved in 3% of the measurement configurations of the Monte Carlo
485 simulation in the open valve-open pump scenario, and this percentage changes to 3.3% and 1.5%
486 in the open valve-closed pump and closed valve-closed pump cases, respectively. In most of these
487 scenarios, the reason why the algorithm achieves k_{max} is that there is an oscillation between $b_{6,8}^P = 0$
488 and $b_{6,8}^P = 1$ along the iterative process. The relative error of the objective function between these
489 two possibilities is in all cases lower than 10%, i.e. the noise of the measurements is such that
490 there is a negligible difference between considering the pump open or closed. This phenomenon

491 disappears when a fourth flow meter is added, thus it can be concluded that even though the system
492 is observable when there is no information about the characteristic curve of the pump, the algorithm
493 may find it difficult to converge if there are few metering devices subjected to a significant noise.
494 Such limitation comes from the nature of the measurements rather than from the method itself.
495 Regardless of this situation, the mean time for each TSE remains between 2 and 3.5 s.

496 **C-TOWN CASE STUDY**

497 In this section, the algorithm for TSE is tested in the well-known C-Town case study, firstly pre-
498 sented in the so called “Battle of Background Leakage Assessment for water networks” (Giustolisi
499 et al. 2014). This system presents 1 reservoir, 7 tanks, 388 nodes, 432 pipes, 11 pumps (grouped
500 in 5 pumping stations S1, S2, S3, S4 and S5), 1 gate valve, and 1 check valve. In this work, we
501 consider the steady state of the network, neglecting the demand patterns and controls provided
502 when the problem was first posed for leakage detection purposes.

503 This water system is here tested under two different assumptions for TSE purposes: (1) in-
504 formation about the characteristic curves of the 11 existing pumps is known, and (2) there is no
505 information about the characteristic curve of any of them. In each of them, three measurement
506 settings are considered. Firstly, we assume that only water levels are metered and demands at
507 junction nodes are pseudomeasured. Secondly, flow meters are added at four of the eight pipes
508 that come out of the tanks and the reservoir in the system, more specifically, at the ones associated
509 with the highest flows. Finally, four additional flow meters (eight in total) are included in the rest
510 of entrances to the network. For each of these measurement settings, we synthetically generate
511 measurements as in the illustrative example, assuming the same standard deviations. In this case,
512 only two network topologies are considered for the artificial generation of measurements in each
513 of the settings: firstly all pumps are working, the gate valve is open and the check valve is closed
514 to avoid inverse flow, and secondly pumps PU1, PU4, PU6 and PU10 are closed, i.e. one pump
515 is closed in pumping stations S1, S2, S3 and S5. As before, the TSE algorithm is initialised from
516 the flow network solution associated with everything opened subjected to a 5% noise. Moreover, a
517 Monte Carlo simulation of 1000 measurement configurations is applied to each of such topologies

518 and measurement settings. We assume the same model parameters as the illustrative example.

519 **Known characteristic curves**

520 Table 3 shows TSE results for the network topologies and measurement settings considered
521 when the characteristic curve of all pumps is known. This table provides the percentage of success
522 in determining the number of pumps working in each pumping station ($S_{P_{Si}}$; $\forall i = 1, 2, 3, 4, 5$), the
523 percentage of success in determining the status of the gate valve (S_{GV}) and the check valve (S_{CV}), the
524 mean (\bar{k}) and maximum ($\max(k)$) number of iterations required for the algorithm to converge, the
525 mean squared error of flows over the 1000 simulations (\overline{MSE}), and the time required to undertake
526 the sampling experiment in the aforementioned desktop computer. The success criterion for pumps
527 is now to correctly determine the number of pumps working per pumping station rather than
528 correctly estimating the status of each individual pump, because all the pumps in each pumping
529 station present the same characteristic curve.

530 This table shows that the status of the pumps and valves in the system cannot be determined with
531 certainty when only water levels at reservoirs and water consumptions are measured. Even though
532 the system is observable under such configuration, measurement inaccuracy does not enable a good
533 TSE. Status estimation is specially bad for $S_{P_{Si}}$; $\forall i = 1, 2, 3, 4, 5$, whereas S_{GV} and S_{CV} remain above
534 80% no matter the real status of the system. S_{GV} and S_{CV} present the same values when all pumps are
535 working and when some of them are not, because the same water level and demand measurements
536 apply. The situation considerably improves when 4 or 8 flow meters are added. In both cases,
537 the number of working pumps and the status of the valves are inferred correctly in all Monte
538 Carlo simulations. As before, \overline{MSE} is considerably reduced with the addition of measurements,
539 i.e. a better estimation can be obtained when metering devices are added. This improvement is
540 higher when four flow meters are added, and lower for the next four extra flow meters. This fact
541 highlights the importance of having redundant measurements, i.e. more measurements than the
542 strictly required to make the system observable, to counteract measurement inaccuracy.

543 On the other hand, it is worth mentioning that \bar{k} and $\max(k)$ are not significantly increased with
544 respect to the illustrative example network, and the average time for each TSE remains 3-4 s, i.e.

545 the algorithm has potential for real time implementation. In this regard, we want to highlight that
546 the aim of this work is to present a methodology that enables to infer both the network topology
547 and hydraulic state of the system from the available measurements, but additional issues must be
548 explored with view to its on-line implementation. For example, hydraulic uncertainty is unavoidable
549 in real-time scenario, thus the hydraulic model needs to be periodically updated in order for TSE
550 to be reliable. Recently, Díaz et al. (2017a) have proposed a calibration method to adjust model
551 parameters based on multi-period state estimation results. Also, demand estimation in real-time
552 is challenging since most large networks have limited data that can be used to estimate demands.
553 This is the main reason why state estimation techniques have not been systematically applied to
554 water systems on an operational level yet, and the only real applications are all related to water
555 transport networks (González et al. 2017; Vrachimis et al. 2016). Water transport networks are
556 pipeline systems that provide water to distinct District Metered Areas (DMA), where incoming flows
557 are normally monitored. Hence, in this type of systems demand uncertainty can be considerably
558 reduced. Further research should apply the methodology here proposed to a real system, as there are
559 always aspects that the model has not reflected and that may introduce errors in the determination of
560 the states of the elements. Additionally, sensitivity analysis, leak detection strategies and uncertainty
561 evaluation should be progressively incorporated to TSE in order to address the on-line monitoring
562 issue in all its complexity (Díaz 2017). In this regard, explicit expressions for state estimation
563 sensitivity analysis have been recently proposed (Díaz et al. 2017c) to further the understanding of
564 state estimation solutions.

565 **Unknown characteristic curves**

566 Table 4 provides the same results when the characteristic curves of the pumps in the system
567 are considered unknown. It must be highlighted that such assumption leads to an unobservable
568 system for all scenarios, and this implies that state estimation results cannot be trusted (Díaz et al.
569 2017b). It is worth mentioning that some high percentages of S_P , S_{GV} and S_{CV} are obtained in
570 some of the configurations, but they must not be relied upon, as they are mere coincidence. This
571 justifies the inconsistencies between Tables 3 and 4 in terms of \overline{MSE} . These results highlight the

572 importance of observability analysis techniques, without which we would just believe the results
573 of the TSE algorithm gathered in Table 4. For this reason, topological observability analysis is a
574 prior necessary step that enables to pre-assess the suitability of measurement configurations.

575 To finish with, we want to highlight that these last scenarios in which no information about the
576 characteristic curves of pumps is available, few meters exist, and all pumps and valves statuses are
577 to be determined, are not consistent with the reality of current water systems. For example, system
578 outflows are metered rather than pseudomeasured in actual water transport networks that provide
579 water to DMAs. Moreover, the characteristic curve of most pumps is normally known, and even
580 many of the statuses of the pumps and valves in the network are known thanks to the existence of
581 position sensors in many controlling devices. This implies that their binary variables can be fixed
582 and only some unknown statuses need to be inferred, thus reducing the complexity of the original
583 MINLP problem. The aim of these examples is to show that the methodology proposed in this
584 paper is robust and can be used in conjunction with observability analysis techniques to assess the
585 behaviour of the system in real-time even when changes in the network topology take place.

586 **CONCLUSIONS**

587 In this work, the importance of undertaking TSE rather than traditional SE is highlighted, and
588 a novel methodology for TSE is presented. Implementing TSE rather than traditional SE permits
589 to drop the assumption that the network topology is known beforehand, enabling to infer both the
590 pump and valve status and the hydraulic state of the system from available measurements. This is of
591 utmost importance at present, as changes in the network topology may take place in order to improve
592 the quality of the supply service and the system reliability. TSE complements available techniques
593 for topological observability analysis, as it permits to take into account measurement noise when
594 estimating pump/valve status rather than only analysing if sufficient algebraic relationships exist.

595 The method for TSE has been set out as a MINLP problem, where the presence of pumps
596 and valves is simulated through binary variables. Due to the complexity of developing a robust
597 method for solving such a challenging problem, it has been here transformed into an iterative MIQP
598 problem by linearizing Hazen-Williams headloss equations and the characteristic curves of pumps.

599 Only pumps, gate valves and check valves have been introduced in this work as controlling devices,
600 but additional hydraulic constraints could be similarly added to the optimisation problem in order
601 to simulate the presence of other types of valves.

602 The proposed methodology has proven to work robustly in conjunction with topological ob-
603 servability analysis in an illustrative example and a larger case study. Different hypotheses have
604 been tested about the information available in the network and the number of metering devices,
605 showing that the approach is versatile and can track changes in the topology even when there
606 is no information about the characteristic curve of an individual pump or group of pumps. The
607 computational cost of the new algorithm proves that it has potential for on-line implementation,
608 although several related issues must be addressed before its real-time application (e.g. hydraulic
609 uncertainty, sensitivity analysis). Additionally, it could constitute a powerful tool when used to
610 train network operators on how to respond to incidences. Furthermore, it could be used as a basis
611 on which other methods for optimal meter placement could be based, not only assessing the best
612 location for additional devices, but also taking into account the possibility of installing position
613 sensors, which would fix the binary variables thus reducing the complexity of the problem. These
614 are subjects for further research.

615 REFERENCES

- 616 Andersen, J. H. and Powell, R. S. (2000). “Implicit state-estimation technique for water network
617 monitoring.” *Urban Water*, 2(2), 123–130.
- 618 Andersen, J. H., Powell, R. S., and Marsh, J. F. (2001). “Constrained state estimation with applica-
619 tions in water distribution network monitoring.” *Int. J. Syst. Sci.*, 32(6), 807–816.
- 620 Bargiela, A. (1984). “On-line monitoring of water distribution networks.” Ph.D. thesis, Univ. of
621 Durham, UK.
- 622 Bargiela, A. and Hainsworth, G. D. (1989). “Pressure and flow uncertainty in water systems.” *J.*
623 *Water Resour. Plann. Manage.*, 115(2), 212–229.
- 624 Berthold, T. (2014). “Heuristic algorithms in global MINLP solvers.” Ph.D. thesis, Technical Univ.
625 of Berlin, Germany.

626 Brdys, M. A. and Chen, K. (1993). “Joint state and parameter estimation of dynamic water supply
627 systems with unknown but bounded uncertainty.” *Integrated Computer Applications in Water*
628 *Supply*, B. Coulbeck, ed., Vol. 1, Research Studies Press, Baldock, UK, 335–355.

629 Brdys, M. A. and Ulanicki, B. (2002). *Operational control of water systems: Structures, algorithms*
630 *and applications*. Prentice Hall, London, UK.

631 Bussieck, M. R. and Vigerske, S. (2011). “MINLP solver software.” *Wiley Encyclopedia of Oper-*
632 *ations Research and Management Science*, John Wiley & Sons, Published online.

633 Carpentier, P. and Cohen, G. (1991). “State estimation and leak detection in water distribution
634 networks.” *Civ. Eng. Syst.*, 8(4), 247–257.

635 Coulbeck, B. (1977). “Optimisation and modelling techniques in dynamic control of water distri-
636 bution systems.” Ph.D. thesis, Univ. of Sheffield, UK.

637 Deuerlein, J. W., Simpson, A. R., and Dempe, S. (2009). “Modeling the behavior of flow regulating
638 devices in water distribution systems using constrained nonlinear programming.” *J. Hydraul.*
639 *Eng.*, 135(11), 970–982.

640 Díaz, S. (2017). “Comprehensive approach for on-line monitoring water distribution systems via
641 state estimation related techniques.” Ph.D. thesis, Univ. of Castilla-La Mancha, Spain.

642 Díaz, S., González, J., and Mínguez, R. (2016). “Observability analysis in water transport networks:
643 Algebraic approach.” *J. Water Resour. Plann. Manage.*, 142(4), 04015071.

644 Díaz, S., González, J., and Mínguez, R. (2016a). “Uncertainty evaluation for constrained state
645 estimation in water distribution systems.” *J. Water Resour. Plann. Manage.*, 142(12), 06016004.

646 Díaz, S., Mínguez, R., and González, J. (2016b). “Stochastic approach to observability analysis in
647 water networks.” *Ingeniería del Agua*, 20(3), 139–152.

648 Díaz, S., Mínguez, R., and González, J. (2017a). “Calibration via multi-period state estimation in
649 water distribution systems.” *Water Resour. Manage.*, doi: 10.1007/s11269-017-1779-2.

650 Díaz, S., Mínguez, R., and González, J. (2017b). “Topological observability analysis in water
651 distribution systems.” *J. Water Resour. Plann. Manage.*, 143(5), 06017001.

652 Díaz, S., Mínguez, R., González, J. and Savic, D. (2017c). “Explicit expressions for state

653 estimation sensitivity analysis in water systems.” *J. Water Resour. Plann. Manage.*, doi:
654 10.1061/(ASCE)WR.1943-5452.0000914.

655 Eck, B. J. and Mevissen, M. (2012). “Valve placement in water networks: Mixed-integer non-linear
656 optimization with quadratic pipe friction.” *IBM Research Report RC25307, Dublin, Ireland.*

657 Gabrys, B. and Bargiela, A. (1996). “Integrated neural based system for state estimation and con-
658 fidence limit analysis in water networks.” *Proceedings of the European Simulation Symposium,*
659 *Genoa, Italy*, 2, 398–402.

660 Giustolisi, O., Berardi, L., Laucelli, D., Savic, D., Walski, T., and Brunone, B. (2014). “Battle of
661 background leakage assessment for water networks (BBLAWN) at WDSA Conference 2014.”
662 *Procedia Eng.*, 89, 4–12.

663 Giustolisi, O., Kapelan, Z., and Savic, D. (2008). “Algorithm for automatic detection of topological
664 changes in water distribution networks.” *J. Hydraul. Eng.*, 134(4), 435–446.

665 González, J., Mínguez, R., and Díaz, S. (2017). *Observability study for hydraulic state estimation*
666 *of the sectorised water supply network. Booklet Research, Development and Innovation 23.* In
667 edition. Canal de Isabel II Gestión, S.A., Madrid, Spain.

668 Goulter, I. (1995). “Analytical and simulation models for reliability analysis in water distribution
669 systems.” *Improving efficiency and reliability in water distribution systems*, E. Cabrera and A. F.
670 Vela, eds., Kluwer Academics, London, UK, 235–266.

671 Irving, M. R., Owen, R. C., and Sterling, M. J. H. (1978). “Power-system state estimation using
672 linear programming.” *Proceedings of the Institution of Electrical Engineers*, 125(9), 879–885.

673 Kumar, S. M., Narasimhan, S., and Bhallamudi, S. M. (2008). “State estimation in water distribution
674 networks using graph-theoretic reduction strategy.” *J. Water Resour. Plann. Manage.*, 134(5),
675 395–403.

676 Lansley, K. E. and Basnet, C. (1991). “Parameter estimation for water distribution networks.” *J.*
677 *Water Resour. Plann. Manage.*, 117(1), 126–144.

678 Laucelli, D., Berardi, L., Giustolisi, O., Vamvakeridou-Lyroudia, L. S., Kapelan, Z., Savic, D., and
679 Barbaroand, G. (2011). “Calibration of water distribution systems using topological analysis.”

680 *12th Annual Conference on Water Distribution Systems Analysis (WDSA), Tucson, USA, 1664–*
681 *1681.*

682 Liberatore, S. and Sechi, G. M. (2009). “Location and calibration of valves in water distribution
683 networks using a scatter-search meta-heuristic approach.” *Water Resour. Manage.*, 23(8), 1479–
684 1495.

685 Morsi, A., Geissler, B., and Martin, A. (2012). “Mixed integer optimization of water supply
686 networks.” *Mathematical optimization of water networks*, A. Martin, K. Klamroth, J. Lang, G.
687 Leugering, A. Morsi, M. Oberlack, M. Ostrowski, and R. Rosen, eds., Springer Basel, Basel,
688 Switzerland, 35–54.

689 Nagar, A. K. and Powell, R. S. (2000). “Observability analysis of water distribution systems under
690 parametric and measurement uncertainty.” *Build. Partnerships*, 1–10.

691 Powell, R. S., Irving, M. R., and Sterling, M. J. H. (1988). “A comparison of three real-time state
692 estimation methods for on-line monitoring of water distribution systems.” *Computer Applications*
693 *in Water Supply*, B. Coulbeck, ed., Vol. 1, Research Studies Press, Taunton, UK, 333–348.

694 Schweppe, F. C. and Wildes, J. (1970). “Power system static-state estimation, Part I: Exact model.”
695 *IEEE Trans. Power Appar. Syst.*, PAS-89(1), 120–125.

696 Sophocleous, S., Savic, D. A., Kapelan, Z., and Giustolisi, O. (2016). “A two-stage calibration
697 for detection of leakage hotspots in a real water distribution network.” *18th Water Distribution*
698 *Systems Analysis, Cartagena, Colombia.*

699 Sterling, M. J. H. and Bargiela, A. (1984). “Minimum norm state estimation for computer control
700 of water distribution systems.” *IEE Proc.*, 131(2), 57–63.

701 Vrachimis, S. G., Eliades, D. G., and Polycarpou, M. M. (2016). “Real-time hydraulic interval
702 state estimation for water transport networks: A case study.” *14th International Computing and*
703 *Control for the Water Industry (CCWI) Conference, Amsterdam, The Netherlands.*

704 Wright, R., Abraham, E., Parpas, P., and Stoianov, I. (2015). “Control of water distribution networks
705 with dynamic DMA topology using strictly feasible sequential convex programming.” *Water*
706 *Resour. Res.*, 51(12), 9925–9941.

707
708
709
710
711
712
713
714
715

List of Tables

1	TSE results for 1000 Monte Carlo sampling experiments in the illustrative example network: known characteristic curve	29
2	TSE results for 1000 Monte Carlo sampling experiments in the illustrative example network: unknown characteristic curve	30
3	TSE results for 1000 Monte Carlo sampling experiments in C-Town case study: known characteristic curve	31
4	TSE results for 1000 Monte Carlo sampling experiments in C-Town case study: unknown characteristic curve	32

TABLE 1. TSE results for 1000 Monte Carlo sampling experiments in the illustrative example network: known characteristic curve

Case	Parameters	Measurement configuration: 3 flow meters	Measurement configuration: 4 flow meters
Open valve Open pump	S_P (%)	61.8	100
	S_{GV} (%)	100	100
	\bar{k}	6.0890	6.1530
	$\max(k)$	26	44
	\overline{MSE} (m ⁶ /h ²)	1.1776e3	1.8999e2
	Time for 1000 simulations (s)	3.0442e3	2.6467e3
Open valve Closed pump	S_P (%)	73.9	100
	S_{GV} (%)	100	100
	\bar{k}	5.5500	5.2980
	$\max(k)$	28	26
	\overline{MSE} (m ⁶ /h ²)	1.2199e3	1.9406e2
	Time for 1000 simulations (s)	2.5596e3	2.5725e3
Closed valve Open pump	S_P (%)	79.9	100
	S_{GV} (%)	100	100
	\bar{k}	3.6750	5.1060
	$\max(k)$	6	7
	\overline{MSE} (m ⁶ /h ²)	2.1496e3	2.0453e2
	Time for 1000 simulations (s)	2.4007e3	2.5176e3
Closed valve Closed pump	S_P (%)	92.0	100
	S_{GV} (%)	100	100
	\bar{k}	2.2650	2.0130
	$\max(k)$	5	5
	\overline{MSE} (m ⁶ /h ²)	2.0227e3	3.2767e2
	Time for 1000 simulations (s)	2.2927e3	2.2792e3

TABLE 2. TSE results for 1000 Monte Carlo sampling experiments in the illustrative example network: unknown characteristic curve

Case	Parameters	Measurement configuration: 3 flow meters	Measurement configuration: 4 flow meters
Open valve Open pump	S_P (%)	68.5	100
	S_{GV} (%)	100	100
	\bar{k}	13.6280	5.8170
	$\max(k)$	100	28
	\overline{MSE} (m ⁶ /h ²)	2.3341e3	2.0352e2
	Time for 1000 simulations (s)	3.3303e3	2.6164e3
Open valve Closed pump	S_P (%)	64.9	98.8
	S_{GV} (%)	100	100
	\bar{k}	10.7860	5.3150
	$\max(k)$	100	26
	\overline{MSE} (m ⁶ /h ²)	1.9212e3	1.9410e2
	Time for 1000 simulations (s)	3.1276e3	2.6472e3
Closed valve Open pump	S_P (%)	95.3	100
	S_{GV} (%)	100	100
	\bar{k}	4.8240	2.9730
	$\max(k)$	9	5
	\overline{MSE} (m ⁶ /h ²)	2.6955e3	3.0500e2
	Time for 1000 simulations (s)	2.6066e3	2.3710e3
Closed valve Closed pump	S_P (%)	53.7	98.8
	S_{GV} (%)	100	100
	\bar{k}	6.5030	2.0420
	$\max(k)$	100	5
	\overline{MSE} (m ⁶ /h ²)	2.0565e3	3.2768e2
	Time for 1000 simulations (s)	2.7773e3	2.3212e3

TABLE 3. TSE results for 1000 Monte Carlo sampling experiments in C-Town case study: known characteristic curve

Case	Parameters	Measurement configuration: no flow meters	Measurement configuration: 4 flow meters	Measurement configuration: 8 flow meters
Open GV Closed CV Open pumps	$S_{P_{S1}}$ (%)	0.0	100	100
	$S_{P_{S2}}$ (%)	0.4	100	100
	$S_{P_{S3}}$ (%)	0.0	100	100
	$S_{P_{S4}}$ (%)	0.0	100	100
	$S_{P_{S5}}$ (%)	0.1	100	100
	S_{GV} (%)	96.3	100	100
	S_{CV} (%)	83.0	100	100
	\bar{k}	2.9160	4.0830	3.9990
	$\max(k)$	13	6	5
	\overline{MSE} (m ⁶ /h ²)	5.0407e4	2.2044	1.5199
Time for 1000 simulations (s)	3.0164e3	3.2103e3	4.2936e3	
Open GV Closed CV Some closed pumps	$S_{P_{S1}}$ (%)	0.3	100	100
	$S_{P_{S2}}$ (%)	7.8	100	100
	$S_{P_{S3}}$ (%)	0.1	100	100
	$S_{P_{S4}}$ (%)	0.0	100	100
	$S_{P_{S5}}$ (%)	3.1	100	100
	S_{GV} (%)	96.3	100	100
	S_{CV} (%)	83.0	100	100
	\bar{k}	2.9160	5.7030	5.0480
	$\max(k)$	13	10	6
	\overline{MSE} (m ⁶ /h ²)	3.3290e4	2.3889	1.5028
Time for 1000 simulations (s)	3.0233e3	3.5202e3	4.4427e3	

TABLE 4. TSE results for 1000 Monte Carlo sampling experiments in C-Town case study: unknown characteristic curve

Case	Parameters	Measurement configuration: no flow meters	Measurement configuration: 4 flow meters	Measurement configuration: 8 flow meters
Open GV Closed CV Open pumps	$S_{P_{S1}}$ (%)	0.0	0.0	0.0
	$S_{P_{S2}}$ (%)	0.0	0.0	0.0
	$S_{P_{S3}}$ (%)	0.0	0.0	0.0
	$S_{P_{S4}}$ (%)	0.0	0.0	0.0
	$S_{P_{S5}}$ (%)	0.0	0.0	0.0
	S_{GV} (%)	98.0	100	100
	S_{CV} (%)	83.1	100	100
	\bar{k}	2.8220	12.8430	4.1860
	$\max(k)$	14	100	15
	\overline{MSE} (m ⁶ /h ²)	4.8366e4	1.1997e3	6.4974
Time for 1000 simulations (s)	2.9525e3	5.8960e3	3.4802e3	
Open GV Closed CV Some closed pumps	$S_{P_{S1}}$ (%)	0.8	81.3	99.9
	$S_{P_{S2}}$ (%)	1.0	100	100
	$S_{P_{S3}}$ (%)	0.0	100	100
	$S_{P_{S4}}$ (%)	0.0	0.0	0.0
	$S_{P_{S5}}$ (%)	0.0	4.6	100
	S_{GV} (%)	98.0	100	100
	S_{CV} (%)	83.1	100	100
	\bar{k}	2.8220	2.8600	5.5760
	$\max(k)$	14	14	17
	\overline{MSE} (m ⁶ /h ²)	3.1292e4	5.1755e2	6.3411
Time for 1000 simulations (s)	2.9742e3	3.2190e3	3.8039e3	

716 **List of Figures**

717 1 Scenarios within a pump element: positive and negative flow 34

718 2 Flow chart for TSE: Iterative linearization approach 35

719 3 Available flow meters at different measurement configurations 36

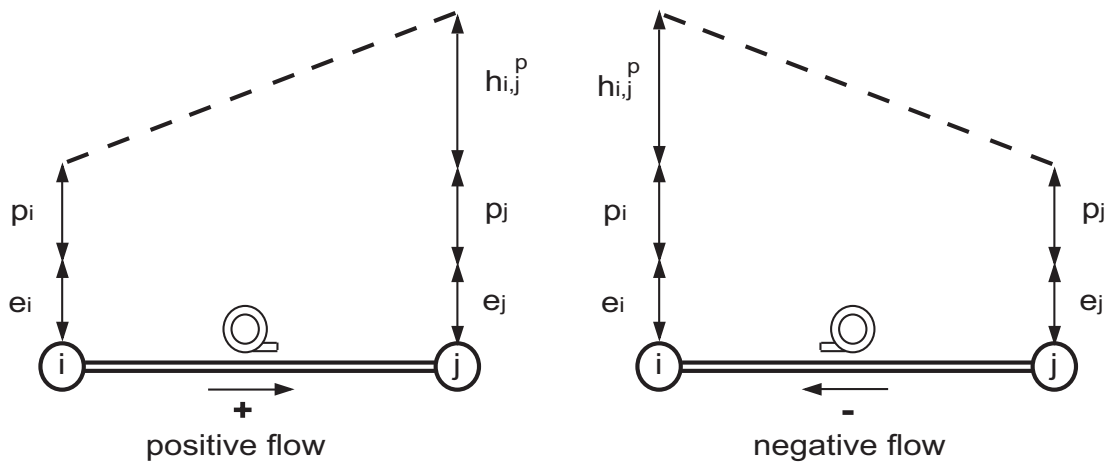


Fig. 1. Scenarios within a pump element: positive and negative flow

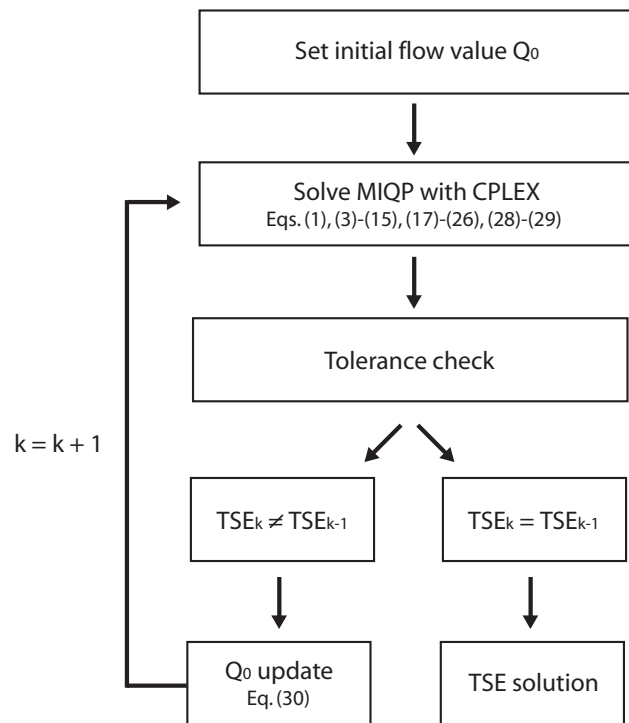


Fig. 2. Flow chart for TSE: Iterative linearization approach

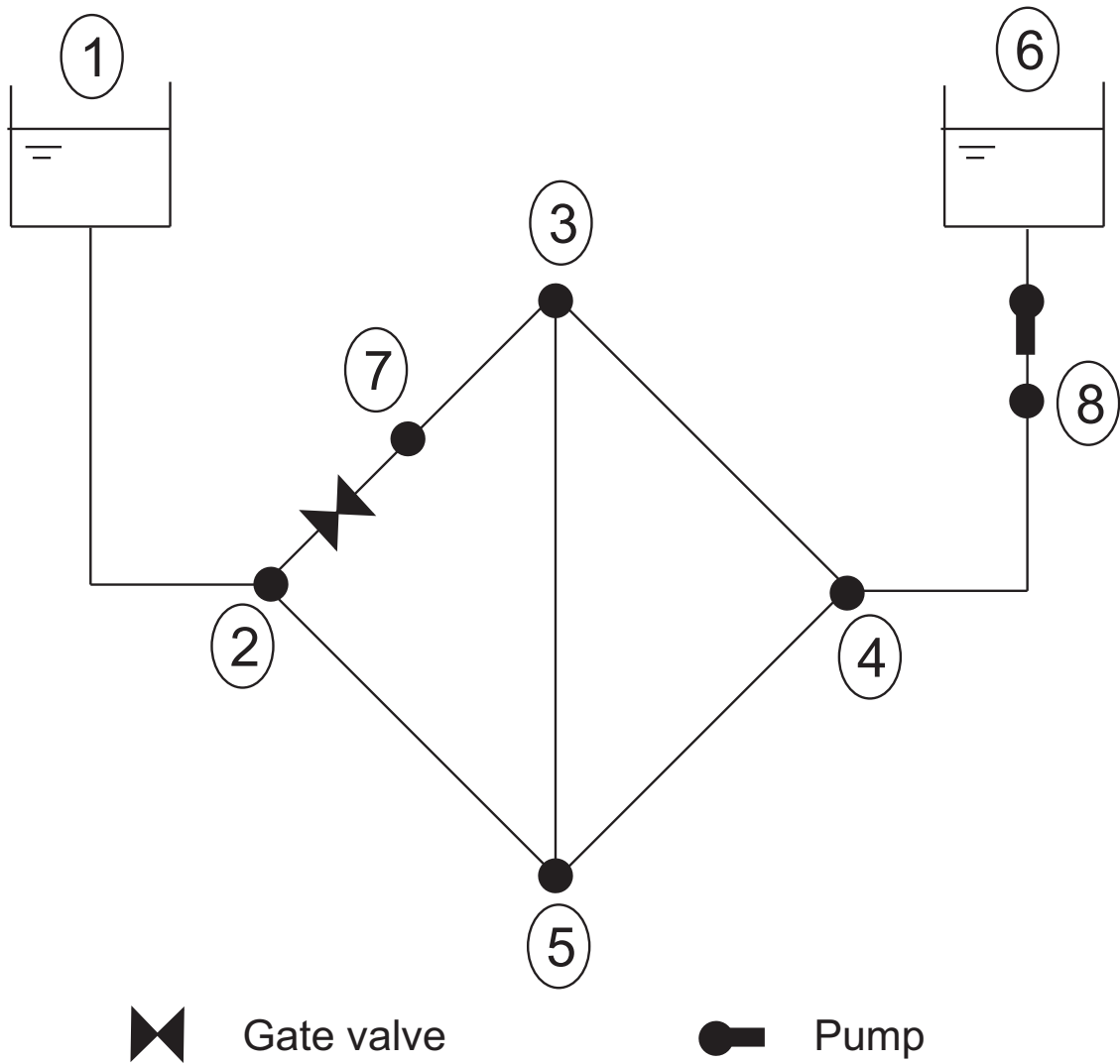


Fig. 3. Available flow meters at different measurement configurations